Inorg. Chem. **2005**, *44*, 8469–8475

Reductive Nitrosylation and Proton-Assisted Bridge Splitting of a (μ-Oxo)dimanganese(III) Complex Derived from a Polypyridine Ligand with One Carboxamide Group

Kaushik Ghosh,[†] Aura A. Eroy-Reveles,[†] Marilyn M. Olmstead,[‡] and Pradip K. Mascharak*,[†]

Department of Chemistry and Biochemistry, University of California, Santa Cruz, California 95064, and Department of Chemistry, University of California, Davis, California 95616

Received March 7, 2005

Aerobic oxidation of the Mn(II) complex $[Mn(Papy_3)(H_2O)](ClO_4)$ (**1**, $PaPy_3^-$ is the anion of the designed ligand *N*,*N*-bis(2-pyridylmethyl)amine-*N*-ethyl-2-pyridine-2-carboxamide) in acetonitrile affords the (μ-oxo)dimanganese(III) complex $[(Mn(PaPy_3))_2(\mu\text{-}O)](ClO_4)_2$ (**3**) in high yield. The unsupported single oxo bridge between the two high-spin Mn(III) centers in **3** is readily cleaved upon addition of proton sources such as phenol, acetic acid, and benzoic acid, and complexes of the type $[Mn(PaPy_3)(L)](ClO_4)$ (**5**, L = PhO^-; **6**, L = AcO^-; **7**, L = BzO^-) are formed. The basicity of the bridge is evident by the fact that simple addition of methanol to a solution of **3** in acetonitrile affords the methoxide complex $[Mn(PaPy_3)(OMe)](ClO_4)$ (**4**). The structures of **3**–**5** and **7** have been determined. Passage of NO through a solution of **3** in acetonitrile produces the $\{Mn\text{–}NO\}^6$ nitrosyl $[Mn(PaPy_3)(NO)](ClO_4)$ (**2**) via reductive nitrosylation. Complexes **4**–**7** also afford the $\{Mn\text{–}NO\}^6$ nitrosyl **2** upon reaction with NO. In the latter case, the anionic O-based ligands (such as MeO^- and PhO^-) act as built-in bases and promote reductive nitrosylation of the Mn(III) complexes.

Introduction

Manganese (Mn) is widely distributed in nature, and among the first-row transition elements, it is second to iron in terms of its natural abundance.[1] In biological systems, manganese not only acts as a Lewis acid like magnesium, zinc, or calcium but also plays important roles in oxidation catalysis like iron and copper, cycling among the oxidation states of +2, +3, and +4. The chemistry of oxo-bridged polynuclear manganese complexes has been investigated in detail because of their potential relevance to Mn-containing catalase and the oxygen-evolving complex (OEC) of photosystem II.[2,3] Although examples of binuclear bis(μ-oxo), bis(μ-carboxylato), and mixed μ-oxo μ-carboxylato complexes of manganese are numerous, a much smaller number of binuclear complexes in which two manganese ions are bridged by a single oxo group have been reported.[3a]

It has recently been recognized that coordination of deprotonated carboxamido nitrogen(s) provides additional stabilization to metal ions in higher oxidation states.[4] Indeed, complexes of Mn(III),[5] Mn(IV),[6] and Mn(V)[7] with coordinated carboxamido nitrogen(s) have been isolated and structurally characterized. Recently, we have reported the

* To whom correspondence should be addressed. E-mail: pradip@chemistry.ucsc.edu.
[†] University of California, Santa Cruz.
[‡] University of California, Davis.

(1) (a) Frausto da Silva, J. J. R.; Williams, R. J. P. *The Biological Chemistry of Elements*. *The Inorganic Chemistry of Life*; Clarendon Press: Oxford, England, 1991. (b) Cotton, F. A.; Wilkinson, G. *Advanced Inorganic Chemistry*; John Wiley & Sons: New York, 1988.
(2) (a) *Manganese Redox Enzymes*; Pecoraro, V. L., Ed.; VCH: New York, 1992. (b) Babcock, G. T. In *New Comprehensive Biochemistry: Photosynthesis*; Amesz, J., Ed.; Elsevier: Amsterdam, 1987; pp 125−158.
(3) (a) Mukhopadhyay, S.; Mandal, S. K.; Bhaduri, S.; Armstrong, W. H. *Chem. Rev.* **2004**, *104*, 3981. (b) Wu, A. J.; Penner-Hahn, J. E.; Pecoraro, V. L. *Chem. Rev.* **2004**, *104*, 903. (c) Renger, G. *Angew. Chem., Int. Ed. Engl.* **1987**, *26*, 643.
(4) (a) Marlin, D. S.; Mascharak, P. K. *Chem. Soc. Rev.* **2000**, *29*, 69. (b) Marlin, D. S.; Olmstead, M. M.; Mascharak, P. K. *Inorg. Chem.* **1999**, *38*, 3258.
(5) (a) Lin, J.; Tu, C.; Lin, H.; Jiang, P.; Ding, J.; Guo, Z. *Inorg. Chem. Commun.* **2003**, *6*, 262. (b) Moreira, R. F.; When, P. M.; Sames, D. *Angew. Chem., Int. Ed.* **2000**, *39*, 1618. (c) Che, C.-M.; Cheng, W.-K. *J. Chem. Soc., Chem. Commun.* **1986**, 1443.
(6) (a) Chandra, S. K.; Chakravorty, A. *Inorg. Chem.* **1992**, *31*, 474. (b) Chandra, S. K.; Choudhury, S. B.; Ray, D.; Chakravorty, A. *J. Chem. Soc., Chem. Commun.* **1990**, 474.
(7) (a) MacDonnell, F. M.; Fackler, N. L. P.; Stern, C.; O'Halloran, T. V. *J. Am. Chem. Soc.* **1994**, *116*, 7431. (b) Collins, T. J.; Powell, R. D.; Slebodnick, C.; Uffelman, E. S. *J. Am. Chem. Soc.* **1990**, *112*, 899.

10.1021/ic0503535 CCC: $30.25
Published on Web 10/13/2005

syntheses of Mn(II) and Mn(III) complexes of a pentadentate ligand ($PaPy_3H$, H is dissociable proton) in which the metal centers are coordinated to one deprotonated carboxamido nitrogen, three pyridyl nitrogens, and a *tert*-amine nitrogen.[8] Studies on the reactivity of these manganese complexes with NO revealed that the Mn(II) complex $[Mn(PaPy_3)(H_2O)](ClO_4)$ (**1**) readily reacts with NO to afford the diamagnetic {Mn−NO}^{6} nitrosyl $[Mn(PaPy_3)(NO)](ClO_4)$ (**2**).[9] This Mn−nitrosyl releases NO when exposed to visible light.[8] Interestingly, the Mn(III) complexes $[Mn(PaPy_3)Cl](ClO_4)$ and $[Mn(PaPy_3)(MeCN)](ClO_4)_2$ do not react with NO.

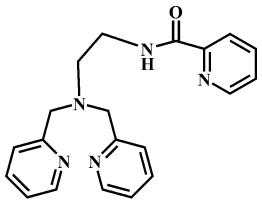

$PaPy_3H$

Coordination of the carboxamido nitrogen to the Mn(II) center in $[Mn(PaPy_3)(H_2O)](ClO_4)$ (**1**) also makes it highly susceptible to oxidation. The beige complex rapidly turns dark brown upon exposure to air. We have now investigated the oxidation reaction, and in this paper we report the spectral and structural characterization of the oxidized product $[(Mn(PaPy_3))_2(\mu\text{-}O)](ClO_4)_2$ (**3**), a binuclear Mn(III) species with a single unsupported oxo bridge. This (μ-oxo)dimanganese(III) complex is an excellent precursor for the synthesis of mononuclear Mn(III) complexes of the type $[Mn(PaPy_3)(L)]^+$ with various LH ligands (H = dissociable proton). The syntheses, structures, and properties of four such complexes namely, $[Mn(PaPy_3)(OMe)](ClO_4)$ (**4**), $[Mn(PaPy_3)(OPh)](ClO_4)$ (**5**), $[Mn(PaPy_3)(OAc)](ClO_4)$ (**6**), and $[Mn(PaPy_3)(OBz)](ClO_4)$ (**7**), are reported herein.

Recent studies on the interactions of NO with the OEC of photosystem II and the Mn-containing catalase have revealed that the oxo-bridged Mn(III,III) units are reduced by NO to Mn(II,III) moieties (and NO^+).[10] Quite in contrast, the present (μ-oxo)dimanganese(III) complex **3** undergoes a novel reductive nitrosylation to afford the previously reported {Mn−NO}^{6} nitrosyl **2**. Although mononuclear iron nitrosyls have been synthesized from oxo-bridged iron porphyrin complexes,[11] to our knowledge, this is the first example of a {Mn−NO}^{6} nitrosyl synthesized from a (μ-oxo)dimanganese(III) species. We further report that the mononuclear Mn(III) complexes **3**−**7** also form the {Mn−NO}^{6} nitrosyl **2** via reductive nitrosylation. This behavior is in contrast to the reported formation of {Mn−NO}^{5} nitrosyls in the reactions of non-porphyrin Mn(III) complexes with NO.[12]

Experimental Section

2-(Aminomethyl)pyridine, *N*-(2-bromoethyl)phthalimide, picolinic acid, hydrazine monohydrate, and $Mn(ClO_4)_2\cdot 6H_2O$ were purchased from Aldrich Chemical Co. and used without further purification. NO gas, procured from Johnson Matthey Chemical Co., was purified by passage through a KOH column. All solvents were distilled from the appropriate drying agents prior to use as follows: DMF from BaO; MeCN and CH_2Cl_2 from CaH_2; MeOH from $Mg(OMe)_2$; Et_2O from Na.

Selected manipulations were carried out using standard Schlenk techniques to avoid exposure to dioxygen.

Caution! Perchlorate salts of metal complexes with organic ligands are potentially explosive. Only small quantities of these compounds should be prepared and handled with proper protection.

Synthesis of the Compounds. The ligand *N*,*N*-bis(2-pyridylmethyl)amine-*N*-ethyl-2-pyridine-2-carboxamide ($PaPy_3H$),[13] $[Mn(DMF)_6](ClO_4)_3$,[14] $[Mn(PaPy_3)(H_2O)](ClO_4)$ (**1**),[8] and $[Mn(PaPy_3)(NO)](ClO_4)$ (**2**)[8] were synthesized by following the published procedures.

$[(Mn(PaPy_3))_2(\mu\text{-}O)](ClO_4)_2$ (3). A batch of 200 mg of $[Mn(PaPy_3)(H_2O)](ClO_4)$ (**1**) was suspended in 10 mL of acetonitrile (MeCN) and stirred for 6 h in the presence of air when a clear deep brown solution was obtained. The solvent was then removed under vacuum, and the resulting brown solid was redissolved in 5 mL of a mixture of dichloromethane (CH_2Cl_2) and MeCN (97:3). Next, hexane (5 mL) was layered on the top of this solution and the mixture was stored at room temperature. Brown crystals were obtained in 55% yield within 2 days. Anal. Calcd for $[(Mn(PaPy_3))_2(\mu\text{-}O)](ClO_4)_2\cdot 2.7CH_2Cl_2\cdot 0.5CH_3CN$ (**3**$\cdot 2.7CH_2Cl_2\cdot 0.5CH_3CN$, $C_{43.70}H_{48.40}Cl_{7.40}Mn_2N_{10.50}O_{11}$): C, 41.36; H, 3.84; N, 11.59. Found: C, 41.82; H, 3.95; N, 11.71. Selected IR frequencies (cm^{-1}, KBr disk): 3585 (m), 3419 (m), 1627 (s, ν_{CO}), 1601 (s), 1480 (m), 1444 (m), 1395 (m), 1293 (m), 1091(s), 1019 (m), 817 (s, μ-O), 759 (m), 689 (m), 623 (m). Electronic absorption spectrum in MeCN, λ_{max} (nm) (ϵ, $M^{-1}\ cm^{-1}$): 715 (260), 547 (475), 260 (28 100).

$[Mn(PaPy_3)(OMe)](ClO_4)$ (4). Method A. A batch of 100 mg of **1** was suspended in a mixture of 10 mL of MeCN and 2 mL of methanol (MeOH), and the mixture was stirred vigorously for 8 h. The reaction mixture gradually became homogeneous during this period. Diffusion of diethyl ether (Et_2O) into the red-brown solution afforded dark red crystals in 80% yield. Anal. Calcd for $[Mn(PaPy_3)(OMe)](ClO_4)$ (**4**, $C_{21}H_{23}ClMnN_5O_6$): C, 47.43; H, 4.36; N, 13.17. Found: C, 47.54; H, 4.39; N, 13.25. Selected IR frequencies (cm^{-1}, KBr disk): 3436 (w), 2802 (w), 1633 (s, ν_{CO}), 1603 (s), 1445 (m), 1389 (m), 1293 (m), 1085 (s), 1023 (m), 765 (m), 690 (m), 623 (m), 558 (m). Electronic absorption spectrum in MeCN, λ_{max} (nm) (ϵ, $M^{-1}\ cm^{-1}$): 710 (115), 540 (185), 260 (12 800). Value of μ_{eff} (298 K, polycryst): 4.54 μ_B.

Method B. A batch of 200 mg (0.58 mmol) of $PaPy_3H$ was dissolved in 10 mL of degassed MeOH, and the solution was stirred with 123 mg (1.2 mmol) of Et_3N for 1 h. Next, a solution of 460 mg (0.58 mmol) of $[Mn(DMF)_6](ClO_4)_3$ in 4 mL of MeOH was added to it, and the reaction mixture was stirred for another 2 h

(8) Ghosh, K.; Eroy-Reveles, A. A.; Avila, B.; Holman, T. H.; Olmstead, M. M., Mascharak, P. K. *Inorg. Chem.* **2004**, *43*, 2988.
(9) The {M−NO}^{n} notation used in this paper is that of Feltham and Enemark. See: Enemark, J. H.; Feltham, R. D. *Coord. Chem. Rev.* **1974**, *13*, 339.
(10) (a) Schansker, G.; Goussias, C.; Petrouleas, V.; Rutherford, A. W. *Biochemistry*, **2002**, *41*, 3057. (b) Ioannidis, N.; Schansker, G.; Barynin, V. V.; Petrouleas, V. *J. Biol. Inorg. Chem.* **2000**, *5*, 354. (c) Sarrou, J.; Ioannidis, N.; Deligiannakis, Y.; Petrouleas, V. *Biochemistry* **1998**, *37*, 3581.
(11) (a) Ellison, M. K.; Schulz, C. E.; Scheidt, W. R. *Inorg. Chem.* **1999**, *38*, 100. (b) Settin, M. F.; Fanning, J. C. *Inorg. Chem.* **1988**, *27*, 1431.
(12) Coleman, W. M.; Taylor, L. T. *J. Am. Chem. Soc.* **1978**, *100*, 1705.
(13) Rowland, J. M.; Olmstead, M. M.; Mascharak, P. K. *Inorg. Chem.* **2001**, *40*, 2810.
(14) Prabhakaran, C. P.; Patel, C. C. *J. Inorg. Nucl. Chem.* **1968**, *30*, 867.

when a red-brown color developed. A batch of 5 mL of Et_2O was then added to it, and the mixture was stored at −20 °C for 24 h. The red-brown microcrystalline product **4** was isolated by filtration, washed with Et_2O, and dried in vacuo (yield: 55%).

Method C. A batch of 100 mg of **3** was suspended in a mixture of 10 mL of MeOH, and the mixture was stirred vigorously for 8 h. The reaction mixture gradually became homogeneous during this period. Diffusion of Et_2O into the red-brown solution afforded dark red crystals in 70% yield.

[Mn(PaPy$_3$)(OPh)](ClO$_4$) (5). Method A. A solution of 30 mg (0.32 mmol) of phenol in 2 mL of MeCN was slowly added to a solution of 200 mg (0.16 mmol) of **3** in 15 mL of MeCN, and the mixture was stirred for 30 min. The initial brown color changed to deep reddish brown during this time. The solvent was then removed and the red-brown solid was recrystallized form CH_2Cl_2/toluene mixture (yield: 80%). Anal. Calcd for [Mn(PaPy$_3$)(OPh)](ClO$_4$) (**5**, $C_{26}H_{25}N_5ClO_6Mn$): C, 52.58; H, 4.24; N, 11.79. Found: C, 52.63; H, 4.28; N, 11.73. Selected IR frequencies (cm^{-1}, KBr disk): 1634 (s, ν_{CO}), 1603 (s), 1482 (m), 1382 (m), 1256 (m), 1085 (s), 1020 (m), 780 (m), 688 (w), 623 (m). Electronic absorption spectrum in MeCN, λ_{max} (nm) (ϵ, M^{-1} cm^{-1}): 460 sh (1 270), 370 sh (3 100), 320 sh (3 850), 260 (14 520). Value of μ_{eff} (298 K, polycryst): 4.92 μ_B.

Method B. A solution of 17 mg (0.69 mmol) of NaH in 2 mL MeCN was slowly added to a solution of 200 mg (0.58 mmol) of PaPy$_3$H in 10 mL of MeCN under dinitrogen. The yellow mixture was stirred for 1 h and then a batch of 460 mg (0.58 mmol) of [Mn(DMF)$_6$](ClO$_4$)$_3$ was added to it. After additional stirring for 2 h, a solution of 73 mg (0.63 mmol) of sodium phenoxide (NaOPh) in 3 mL of MeCN was added to the greenish-brown reaction mixture. This changed the color rapidly to reddish brown. Next, the solvent (MeCN) was removed and the solid was redissolved in 5 mL of CH_2Cl_2. Slow evaporation of the CH_2Cl_2 solution afforded crystalline product in 65% yield.

[Mn(PaPy$_3$)(OAc)](ClO$_4$) (6). Method A. A solution of 22 mg (0.35 mmol) of glacial acetic acid in 2 mL of MeCN was slowly added to a solution of 200 mg (0.16 mmol) of **3** in 10 mL of MeCN when the color rapidly changed from brown to green. Removal of solvent afforded a green microcrystalline solid which was recrystallized from CH_2Cl_2 (yield: 75%). Anal. Calcd for [Mn(PaPy$_3$)(OAc)](ClO$_4$) (**6**, $C_{22}H_{23}N_5MnClO_7$): C, 47.20; H, 4.14; N, 12.51. Found: C, 47.31; H, 4.19; N, 12.44. Selected IR frequencies (cm^{-1}, KBr disk): 1644 (s, ν_{CO}), 1604 (s), 1445 (m), 1367 (s), 1276 (s), 1144 (m), 1085 (s), 795 (m), 761 (m), 677 (m), 625 (m). Electronic absorption spectrum in MeCN, λ_{max} (nm) (ϵ, M^{-1}cm^{-1}): 840 (100), 570 (155), 310 (4 760), 260 (17 000).

Method B. A solution of 17 mg (0.69 mmol) of NaH in 2 mL of MeCN was slowly added to a solution of 200 mg (0.58 mmol) of PaPy$_3$H in 10 mL of MeCN under dinitrogen. The resulting yellow solution was stirred for 1 h, and then a batch of 460 mg (0.58 mmol) of [Mn(DMF)$_6$](ClO$_4$)$_3$ was added to it. Following additional stirring for 2 h, a solution of 52 mg (0.63 mmol) of sodium acetate (NaOAc) in 3 mL of MeCN was added to the greenish brown mixture. The color slowly turned to deep green. Next, the solvent was removed and the green solid was recrystallized from CH_2Cl_2 (yield: 55%).

[Mn(PaPy$_3$)(OBz)](ClO$_4$) (7). Method A. A solution of 40 mg (0.33 mmol) benzoic acid (HOBz) in 2 mL of MeCN was slowly added to a solution of 200 mg (0.16 mmol) of **3** in 15 mL of MeCN. The color of the reaction mixture changed from brown to green within 15 min. Removal of solvent and recrystallization of the green solid from CH_2Cl_2/toluene mixture afforded the complex in yield 80%. Anal. Calcd for [Mn(PaPy$_3$)(OBz)](ClO$_4$)·CH_2Cl_2 (**7**·CH_2Cl_2, $C_{28}H_{27}Cl_3MnN_5O_7$): C, 47.58; H, 3.85; N, 9.90. Found: C, 47.79; H, 3.87; N, 9.94. Selected IR frequencies (cm^{-1}, KBr disk): 1709 (m, ν_{CO} of OBz), 1643 (s, ν_{CO}), 1604 (s), 1444 (m), 1365 (m), 1320 (s) 1300 (s), 1089 (s), 1021 (m), 723 (m), 623 (m). Electronic absorption spectrum in MeCN, λ_{max} (nm) (ϵ, M^{-1} cm^{-1}): 855 (105), 590 (160), 315 (5 700), 260 (19 200). Value of μ_{eff} (298 K, polycryst): 4.90 μ_B.

Method B. A solution of 17 mg (0.69 mmol) of NaH in 2 mL of MeCN was added to a solution of 200 mg (0.58 mmol) of PaPy$_3$H in 10 mL of MeCN under dinitrogen. The yellow mixture was stirred for 1 h, and a batch of 460 mg (0.58 mmol) of [Mn(DMF)$_6$](ClO$_4$)$_3$ was added to it. Following additional stirring for 2 h, a solution of 92 mg (0.64 mmol) of sodium benzoate (NaOBz) in 3 mL of MeCN was added to the reaction mixture. The deep green solution thus obtained was evaporated to dryness, and the green solid was recrystallized from CH_2Cl_2 (yield: 50%).

In this work, complex [Mn(PaPy$_3$)(NO)](ClO$_4$) (**2**) was synthesized by a new procedure. A batch of 200 mg of **3** was dissolved in 15 mL of degassed MeCN, and purified NO gas was passed through the solution for 20 min. The solution was then kept under NO in dark for 24 h. Addition of Et_2O to the dark green solution thus obtained afforded dark green crystals of **2** in 70% yield.

Physical Measurements. Electronic absorption spectra were recorded on a Perkin-Elmer Lambda 9 spectrophotometer. Infrared spectra were obtained with a Perkin-Elmer 1600 or Spectrum 1 FTIR spectrophotometer. ^{1}H NMR spectra were recorded at 298 K on a Varian Unity Plus 500 spectrometer running Solaris 2.6/VNMR 6.1B. A Johnson-Matthey magnetic susceptibility balance was used to determine the room-temperature magnetic susceptibility of **4**, **5**, and **7**·CH_2Cl_2. Dc magnetic susceptibility data for ground [(Mn(PaPy$_3$))$_2$(μ-O)](ClO$_4$)$_2$·2.7CH_2Cl_2·0.5CH_3CN were collected using a Quantum Design MPMS-XL SQUID magnetometer at temperature ranging from 2 to 300 K under an applied magnetic field of 1000 G. Data were corrected for diamagnetic contributions using Pascal's constants.

Gas Chromatographic Analyses. Gas chromatography was performed on a Hewlett-Packard 5890 Series II instrument equipped with a thermal conductivity (TC) detector and a 10 ft Haysep packed column. The column flow rate of He carrier gas was 25 mL/min at 35 °C. Under these conditions, the retention times (min) for various gases were determined as N_2 (0.59), NO (0.69), and NO_2 (2.56). The reaction of **3** with NO was performed in a 20 mL Schlenk flask. A solution of 35 mg of the μ-oxo dimer **3** in 10 mL of MeCN was first degassed thoroughly, and then 4 equiv of purified NO gas was delivered into the flask via a gastight syringe. The solution was then stirred for 16 h. During this time, the color of the solution changed from brown to green. Next, 50 μL of the gas from the headspace was taken out and analyzed by GC.

X-ray Crystal Structure Analysis. Deep purple crystals of [(Mn(PaPy$_3$))$_2$(μ-O)](ClO$_4$)$_2$·2.7CH_2Cl_2·0.5CH_3CN (**3**·2.7CH_2Cl_2·0.5CH_3CN**)** were grown by layering hexane over a solution of the complex in CH_2Cl_2/MeCN (97:3). Reddish crystals of [Mn(PaPy$_3$)(OMe)](ClO$_4$) (**4**) were grown via ether diffusion into a solution of **4** in MeCN at −20 °C. Red crystals of [Mn(PaPy$_3$)(OPh)](ClO$_4$) (**5**) and green crystals of [Mn(PaPy$_3$)(OBz)](ClO$_4$)·CH_2Cl_2 (**7**·CH_2Cl_2**)** were grown by slow evaporation of solutions of the complexes in CH_2Cl_2/toluene (60:40). Diffraction data for **3**−**5** were collected at 90 K on a Bruker SMART 1000 diffractometer while data for **7** were collected at 90 K on a Bruker Apex CCD diffractometer. Mo Kα (0.710 73 Å) radiation was used, and an absorption correction was applied in each case. The structures were solved by direct methods (SHELXS-97). The intensities of twostandard reflections

Table 1. Summary of Crystal Data and Intensity Collection and Structural Refinement Parameters for $[(Mn(PaPy_3))_2(\mu\text{-}O)](ClO_4)_2 \cdot 2.7CH_2Cl_2 \cdot 0.5CH_3CN$ (**3**·$2.7CH_2Cl_2$·$0.5CH_3CN$), $[Mn(PaPy_3)(OMe)](ClO_4)$ (**4**), $[Mn(PaPy_3)(OPh)](ClO_4)$ (**5**), and $[Mn(PaPy_3)(OBz)](ClO_4) \cdot CH_2Cl_2$ (**7**·CH_2Cl_2)

param	**3**	**4**	**5**	**7**
formula	$C_{43.70}H_{48.40}Cl_{7.40}Mn_2N_{10.50}O_{11}$	$C_{21}H_{23}ClMnN_5O_6$	$C_{26}H_{25}ClMnN_5O_6$	$C_{28}H_{27}Cl_3MnN_5O_7$
mol wt	1268.94	531.83	593.90	706.84
cryst color, habit	purple plate	brown needle	dark red block	green plate
T, K	90(2)	90(2)	90(2)	123(2)
cryst syst	monoclinic	orthorhombic	orthorhombic	triclinic
space group	$C2/c$	$P2_12_12_1$	$P2_12_12_1$	$P\bar{1}$
a, Å	17.112(3)	8.4315(6)	8.5126(6)	11.2904(9)
b, Å	13.682(3)	11.0777(8)	11.2530(7)	17.3599(13)
c, Å	22.511(5)	24.0524(18)	26.6159(17)	17.8750(13)
α, deg	90	90	90	110.209(4)
β, deg	106.344(9)	90	90	105.526(2)
γ, deg	90	90	90	102.543(3)
V, Å^3	5057.5(18)	2246.5(3)	2549.6(3)	2976.3(4)
Z	4	4	4	4
d_{calcd}, g cm^{-3}	1.667	1.572	1.547	1.577
abs coeff, μ, mm^{-1}	0.961	0.756	0.675	0.769
GOF[a] on F^2	1.065	1.021	1.026	0.995
R1,[b] %	6.15	3.14	2.84	5.24
wR2,[c] %	15.60	6.97	6.84	12.50

[a] GOF = $[\Sigma w(F_o^2 - F_c^2)^2]/(M - N)]^{1/2}$ (M = number of reflections; N = number of parameters refined). [b] R1 = $\Sigma||F_o| - |F_c||/\Sigma|F_o|$. [c] wR2 = $[\Sigma[w(F_o^2 - F_c^2)^2]/\Sigma[w(F_o)^2]]^{1/2}$.

Table 2. Selected Bond Distances (Å) and Bond Angles (deg) for $[(Mn(PaPy_3))_2(\mu\text{-}O)](ClO_4)_2 \cdot 2.7CH_2Cl_2 \cdot 0.5CH_3CN$ (**3**·$2.7CH_2Cl_2$·$0.5CH_3CN$), $[Mn(PaPy_3)(OMe)](ClO_4)$ (**4**), $[Mn(PaPy_3)(OPh)](ClO_4)$ (**5**), and $[Mn(PaPy_3)(OBz)](ClO_4) \cdot CH_2Cl_2$ (**7**·CH_2Cl_2)

param	**3**	**4**	**5**	**7**
Mn−N(1)	2.130(4)	2.1192(19)	2.1147(13)	2.127(2)
Mn−N(2)	1.969(4)	1.9488(19)	1.9315(13)	1.925(2)
Mn−N(3)	2.213(4)	2.245(2)	2.2093(13)	2.207(2)
Mn−N(4)	2.206(4)	2.128(2)	2.1821(13)	2.141(2)
Mn−N(5)	2.200(4)	2.1844(19)	2.2183(13)	2.170(2)
Mn−O(2)	1.7886(8)	1.8256(16)	1.8513(11)	1.8987(19)
O(1)−C(6)	1.244(6)	1.240(3)	1.2384(19)	1.229(3)
N(2)−C(6)	1.327(7)	1.332(3)	1.3444(19)	1.341(4)
N(3)−C(15)	1.486(7)	1.480(3)	1.4812(19)	1.485(3)
O(2)−C(21)		1.403(3)	1.3538(19)	1.302(3)
O(3)−C(21)				1.227(3)
Mn−Mn	3.5636(8)			
N(1)−Mn−N(2)	77.76(17)	78.35(8)	78.91(5)	79.00(9)
N(1)−Mn−N(3)	156.83(15)	157.04(8)	159.86(5)	160.53(9)
N(1)−Mn−N(4)	98.55(16)	109.58(8)	105.91(5)	100.44(9)
N(1)−Mn−N(5)	106.50(16)	96.73(8)	101.78(5)	105.31(9)
N(1)−Mn−O(2)	101.43(15)	99.77(8)	97.32(5)	106.31(8)
N(2)−Mn−N(3)	80.19(16)	80.49(7)	81.52(5)	81.53(9)
N(2)−Mn−N(4)	91.35(16)	85.36(8)	86.52(5)	86.47(9)
N(2)−Mn−N(5)	82.43(16)	94.35(8)	94.78(5)	95.40(9)
N(2)−Mn−O(2)	177.23(16)	172.03(8)	173.52(5)	170.93(9)
N(3)−Mn−N(4)	74.87(16)	77.28(7)	77.41(5)	78.44(9)
N(3)−Mn−N(5)	77.33(15)	76.06(7)	75.13(4)	76.29(9)
N(3)−Mn−O(2)	100.93(14)	102.39(8)	102.60(5)	93.02(8)
N(4)−Mn−N(5)	152.16(16)	153.00(7)	151.99(5)	154.07(9)
N(4)−Mn−O(2)	91.39(14)	88.02(7)	89.49(5)	85.33(9)
N(5)−Mn−O(2)	95.32(18)	93.56(7)	91.13(5)	90.30(9)
Mn−O(2)−C(21)		129.81(16)	131.75(10)	127.20(19)
O(2)−C(21)−O(3)				124.1(3)
Mn(1)−O(2)−Mn(1)	173.0(3)			

showed no significant decay during the course of data collection. Machine parameters, crystal data, and data collection parameters are summarized in Table 1, while selected bond distances and angles are listed in Table 2.

Results and Discussion

Syntheses. The deprotonated ligand $PaPy_3^-$ serves as a pentadentate ligand in all complexes reported in this account and employs three pyridine nitrogens, one *tert*-amine nitrogen, and one deprotonated carboxamido nitrogen to bind manganese. Among the manganese complexes of $PaPy_3^-$, the mononuclear Mn(II) species $[Mn(PaPy_3)(H_2O)](ClO_4)$ (**1**) reported previously by this group is sensitive to oxidation in solution.[8] Isolation of this complex under anaerobic condition has been possible because of its insolubility in common solvents such as MeOH and MeCN. When a suspension of **1** in MeCN is exposed to air, the beige insoluble compound gradually goes into the solution and the brown (μ-oxo)dimanganese(III) complex $[(Mn(PaPy_3))_2(\mu\text{-}O)](ClO_4)_2$ (**3**) is formed. Complex **3** is stable in aprotic solvents and exhibits no tendency of disproportionation into Mn(II) and/or Mn(IV) species. However, when a few drops of MeOH are added to a solution of **3** in MeCN, it is rapidly converted into the mononuclear Mn(III) complex $[Mn(PaPy_3)(OMe)](ClO_4)$ (**4**). Complex **4** can also be prepared directly by reacting $[Mn(DMF)_6](ClO_4)_3$ and $PaPy_3H$ in the presence of 2 equiv of Et_3N in MeOH. This reaction presumably proceeds via in situ formation of $[Mn(PaPy_3)(MeOH)]^{2+}$ which is further deprotonated (by Et_3N) to form **4** in high (55%) yield.

Treatment of the (μ-oxo)dimanganese(III) species **3** with phenol, acetic acid, or benzoic acid affords the mononuclear Mn(III) species $[Mn(PaPy_3)(OPh)]ClO_4$ (**5**), $[Mn(PaPy_3)(OAc)]ClO_4$ (**6**), and $[Mn(PaPy_3)(OBz)]ClO_4$ (**7**), respectively. These complexes can be independently synthesized from the mononuclear Mn(III) precursor $[Mn(PaPy_3)(MeCN)]^{2+}$, generated from reaction of deprotonated $PaPy_3^-$ (with NaH) and $[Mn(DMF)_6](ClO_4)_3$ in MeCN. Although all attempts to isolate the intermediate species $[Mn(PaPy_3)(MeCN)]^{2+}$ have failed so far, addition of NaOPh, NaOAc, or NaOBz to this species (formed in situ) has resulted in the formation of complexes **5**−**7**, respectively.

Structure and Properties. $[(Mn(PaPy_3))_2(\mu\text{-}O)](ClO_4)_2 \cdot 2.7CH_2Cl_2 \cdot 0.5CH_3CN$ (3·$2.7CH_2Cl_2$·$0.5CH_3CN$). The structure of $[(Mn(PaPy_3))_2(\mu\text{-}O)]^{2+}$ (the cation of **3**) is shown in Figure 1, and selected bond distances and bond angles are listed in Table 2. In **3**, the coordination of the pentadentate $PaPy_3^-$ ligand is similar to that observed in the mononuclear Mn(III) complex $[Mn(PaPy_3)(Cl)](ClO_4)$ reported previously by this group.[8] The *tert*-amine and three pyridine nitrogens of the ligand comprise the equatorial plane while the carboxamido nitrogen occupies a position trans to the bridging oxide. Both Mn(III) centers exist in distorted octahedral geometry represented by the trans angles of 156.83(15)° for N(1)−Mn−N(3) and 152.16(16)° for N(4)−Mn−N(5). The equatorial plane of each Mn center is almost parallel to the other resulting in the nearly linear Mn−O−Mn angle of 173.0(3)°. All structurally characterized (μ-oxo)-dimanganese(III) complexes contain linear or nearly linear Mn−O−Mn units.[3a] The two Mn centers are equivalent with the halves of the dimer related by a 2-fold axis through the bridging oxygen atom. Comparison of the metric parameters

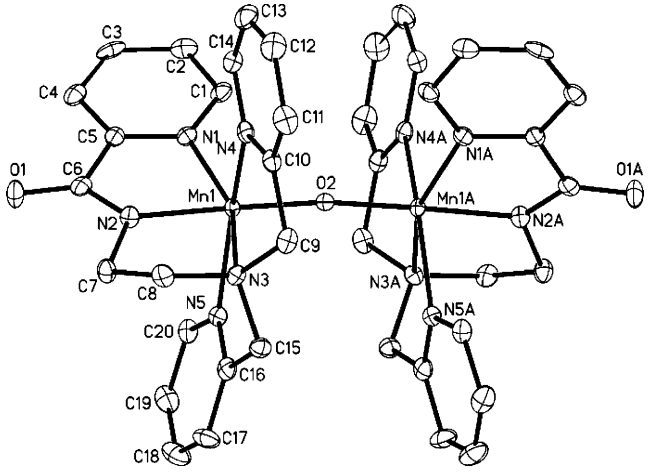

Figure 1. Thermal ellipsoid plot (50% probability level) of the cation of $[(Mn(PaPy_3))_2(\mu\text{-}O)]^{2+}$ (cation of **3**) with the atom-numbering scheme. The hydrogen atoms are omitted for the sake of clarity.

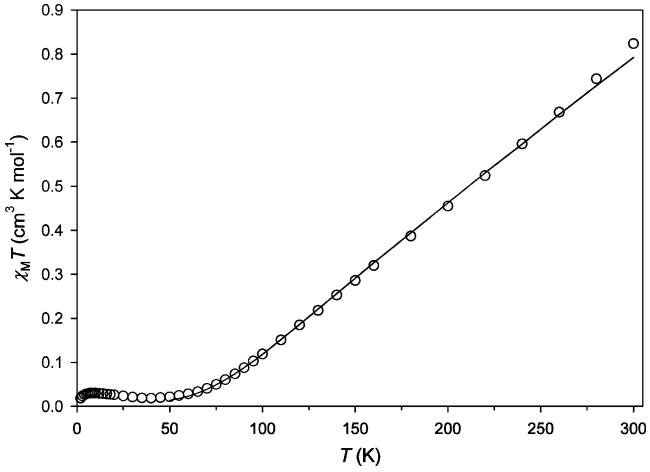

Figure 2. Plot of the product of magnetic susceptibility/mol by temperature ($\chi_M T$) vs temperature (T) for **3**·2.7CH_2Cl_2·0.5CH_3CN. The solid line was generated by the best-fit parameters given in the text.

of $[(Mn(PaPy_3))_2(\mu\text{-}O)]^{2+}$ (Table 2) and $[Mn(PaPy_3)(Cl)]^+$ reveal that the metal−ligand distances of both Mn(III) complexes are relatively similar. For example, the average Mn−N bond distance in the equatorial plane of **3** is 2.187 (4) Å while the same average for $[Mn(PaPy_3)(Cl)](ClO_4)$ (a high-spin complex)[8] is 2.1710 (11) Å. This similarity strongly suggests that the Mn(III) centers in **3** are high-spin. In **3**, the strong trans-influence of the bridging oxo group is clearly reflected in the longer $Mn-N_{amido}$ (Mn−N(2)) bond distance of 1.969(4) Å; in $[Mn(PaPy_3)(Cl)](ClO_4)$ and the following three structures, this distance is considerably shorter (1.9133−1.9488 Å). The Mn−N(2) bond distance of **3** is also longer than the two $Mn-N_{amido}$ bonds in $[Mn(bpb)(H_2O)Cl]$ (1.922-(4) and 1.945(3) Å).[4a] The trans effect of the carboxamido moiety results in a slightly longer Mn−O distance of 1.7886-(8) Å in **3** when compared to other structurally characterized complexes containing the Mn(III)−O−Mn(III) core (1.72−1.77 Å).[3a] The Mn−Mn distance (3.5636 Å) of **3** (calculated from the Mn−O bond distance and the Mn−O−Mn angle) is also longer than all other Mn−O−Mn dimers reported (3.42−3.54 Å), even when compared to complexes with strong field ligands such as CN^-, Pc (phthalocyanate), and TPP (tetraphenylporphyrin).[3a] To our knowledge, this is the first structurally characterized (μ-oxo)dimanganese(III) complex with carboxamido nitrogen coordination. Interestingly, the $Mn-N_{amido}$ (Mn−N(2)) bond of **3** is shorter than the $Fe-N_{amido}$ distance of 2.064(4) Å in the high-spin (μ-oxo)diiron-(III) complex $[(Fe(PaPy_3))_2(\mu\text{-}O)]ClO_4)_2$.[15]

Coordination of the carboxamido nitrogen to Mn(III) in **3** is indicated by the red shift in ν_{CO} frequency from 1666 cm^{-1} in free $PaPy_3H$ to 1627 cm^{-1} in **3**. This value is close to that displayed by mononuclear Mn(III) species presented here with the same pentadentate ligand (1644−1633 cm^{-1}). The μ-oxo bridge displays a strong IR band at 817 cm^{-1}.[16] The molar magnetic susceptibility (χ_M) of **3** (ground crystals) has been measured as a function of the temperature T (2−300 K). The results are shown in Figure 2 in the form of a $\chi_M T$ versus T plot. The $\chi_M T$ value decreases from 0.792 cm^3 mol^{-1} K at 300 K to 0.188 cm^3 K mol^{-1} at 40 K, which is characteristic of a strong antiferromagnetic coupling between the two $S = 2$ high-spin Mn(III) centers. Below 40 K, the $\chi_M T$ values exhibit a small maximum around 10 K (0.03 cm^3 K mol^{-1}) due to paramagnetic Mn(II) impurities. The data above 40 K were fitted with the aid of the program MAGFIT 3.1[17] and an exchange Hamiltonian of the form $\hat{H} = -2J(\hat{S}_1 \cdot \hat{S}_2)$, where $S_1 = S_2 = 2$, to give $g = 2.010$ and $J = -115.8$ cm^{-1}. The magnitude and sign of J for **3** compare well with those of $[Mn_2O(5\text{-}NO_2\text{-saldien})_2]$ ($J = -120.0$ cm^{-1})[18] and $[Mn_2O(bpmsed)_2](ClO_4)_2$ ($J = -108.0$ cm^{-1}),[19] two Mn(III) Schiff base complexes containing a similar linear Mn(III)−O−Mn(III) core.

Mononuclear Mn(III) Complexes. The structures of the cations of $[Mn(PaPy_3)(OMe)]ClO_4$ (**4**), $[Mn(PaPy_3)(OPh)]ClO_4$ (**5**), and $[Mn(PaPy_3)(OBz)]ClO_4$ (**7**) are shown in Figures 3−5, respectively. In these complexes, the mode of coordination of the pentadentate $PaPy_3^-$ ligand is similar to that observed in **3**. The carboxamido nitrogen in each complex is trans to the sixth ligand: MeO^- for **4**; PhO^- for **5**; BzO^- for **7**. Each anionic sixth ligand is coordinated in a monodentate fashion. The metric parameters of the three complexes are comparable to each other (Table 2) and are consistent with the high-spin nature of the Mn(III) centers.[8] Interestingly, the average $Mn-N_{amide}$ distances in the present complexes **4**, **5**, and **7** are comparable to the $Mn-N_{amide}$ distances of 1.922(4) and 1.945(3) Å noted for the dicarboxamido complex $[Mn(bpb)(H_2O)Cl]$.[5a] However, the $Mn-N_{py}$ distance observed in $[Mn(bpb)(H_2O)Cl]$ (2.061(3) Å) is noticeably shorter than the same distance in **4**, **5**, or **7**. The Mn−O(OMe) bond distance in **3** (1.8256(16) Å) is similar

(15) Patra, A. K.; Afshar, R. K.; Rowland, J. M.; Olmstead, M. M.; Mascharak, P. K. *Angew. Chem., Int. Ed.* **2003**, *42*, 4517.
(16) (a) Ziolo, R. F.; Stanford, R. H.; Rossman, G. R.; Gray, H. B. *J. Am. Chem. Soc.* **1974**, *96*, 7910. (b) Schardt, B. C.; Hollander, F. J.; Hill, C. L. *J. Am. Chem. Soc.* **1982**, *104*, 3964.
(17) Schmitt, E. A. Ph.D. Thesis, University of Illinois at Urbana-Champaign, 1995.
(18) Kipke, C. A.; Scott, M. J.; Gohdes, J. W.; Armstrong, W. H. *Inorg. Chem.* **1990**, *29*, 2193.
(19) Horner, O.; Anxolabéhère-Mallart, E.; Charlot, M.-F.; Tchertanov, L.; Guilhem, J.; Mattioli, T. A.; Boussac, A.; Girerd, J.-J. *Inorg. Chem.* **1999**, *38*, 1222.

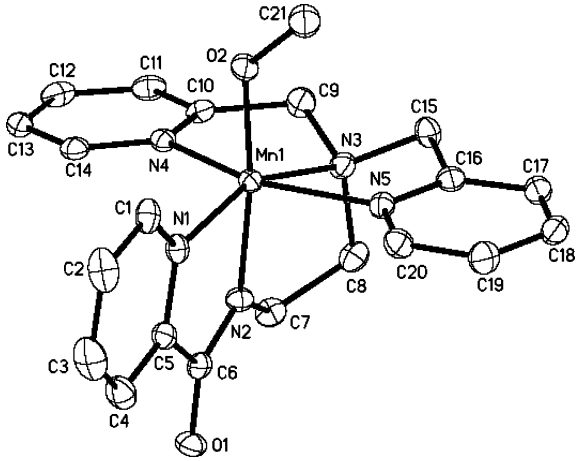

Figure 3. Thermal ellipsoid plot (50% probability level) of cation of $[Mn(PaPy_3)(OMe)]^+$ (cation of **4**) with the atom-numbering scheme. The hydrogen atoms are omitted for the sake of clarity.

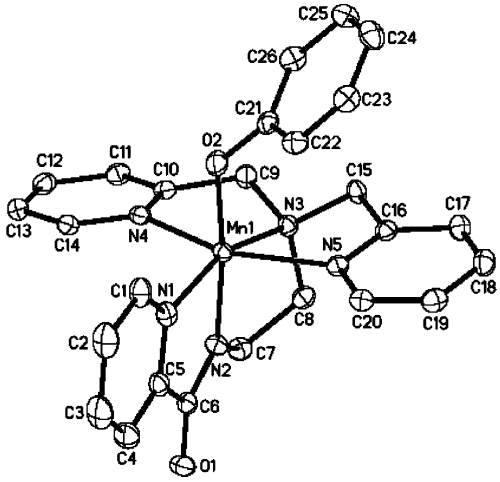

Figure 4. Thermal ellipsoid plot (50% probability level) of cation of $[Mn(PaPy_3)(OPh)]^+$ (cation of **5**) with the atom-numbering scheme. The hydrogen atoms are omitted for the sake of clarity.

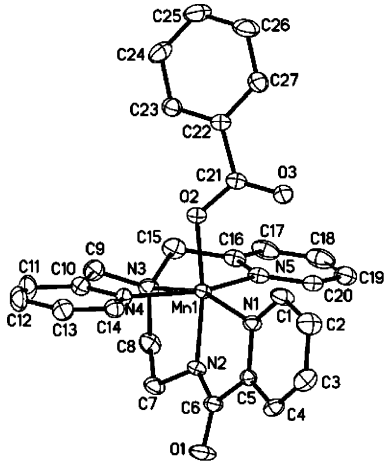

Figure 5. Thermal ellipsoid plot (50% probability level) of cation of $[Mn(PaPy_3)(OBz)]^+$ (cation of **7**) with the atom-numbering scheme. The hydrogen atoms are omitted for the sake of clarity.

to that reported for other Mn(III) complexes such as $[Mn(L)(OMe)_2]PF_6$ (L is a tetraazamacrocycle, Mn−O distance: 1.838(2) Å).[20] Likewise, the Mn−O(OPh) bond length of **5** (1.8513(11) Å) is comparable to that reported for Mn-

Scheme 1

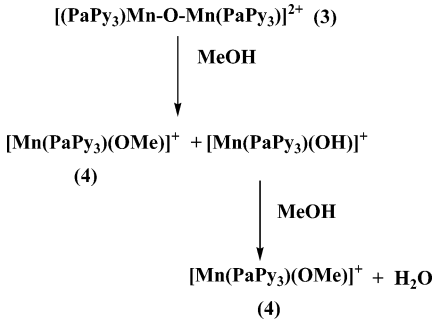

(III) complexes of Schiff base ligands that incorporate phenolate groups such as $[Mn(sal\text{-}N\text{-}1,5,8,12)](ClO_4)$ and $[Mn(salpn)H_2DCBI(DMF)]$ (Mn−O(OPh) distance: 1.869(4) and 1.877(2) Å, respectively).[21]

In **7**, the benzoate ligand is monodentate. To our knowledge, this mode of coordination of benzoate to Mn(III) is unique. The Mn−O(OBz) bond length of 1.8987(19) Å in **7** is shorter than the Mn−O(OBz) distance of 2.083(3) Å observed in $[Mn(piap)(OBz)_2]$, a Mn(II) complex containing two monodentate benzoate ligands.[22] It is interesting to note that the Mn−O(OBz) bond distance of **7** is quite comparable to the Mn−O distance (1.903(3) Å) of the Mn(III) complex $(Et_4N)[MnCl_2(pic)_2]$ that contains the chelating pyridine-2-carboxylate (pic) ligand.[23]

Reactivity of $[(Mn(PaPy_3))_2(\mu\text{-}O)](ClO_4)_2$ (3). Aerobic oxidation of the Mn(II) starting complex $[Mn(PaPy_3)(H_2O)](ClO_4)$ (**1**) in MeCN readily affords **3**, a Mn(III) dimer with a single unsupported oxo bridge. The single μ-oxo bridge in **3** is not stable toward proton donors. Protonation of the μ-oxo bridge results in splitting of the dimer and allows the corresponding anion to bind at the sixth site (trans to the carboxamido N). For example, simple addition of a few drops of MeOH to a solution of **3** in MeCN results in the formation of the monomeric methoxide complex **4**. Similar reactivity is observed with other proton donors such as benzoic acid, acetic acid, and phenol. These reactions can be followed visually since treatment of 1 equiv of the dark brown **3** with 2 equiv of acetic or benzoic acid affords the green acetate complex **6** (λ_{max} = 570 nm) or the green benzoate complex **7** (λ_{max} = 590 nm). Addition of phenol affords the deep red phenolate complex **5** (λ_{max} = 460 nm). Interestingly, addition of NaOAc or NaOPh to a solution of **3** in MeCN does *not* result in a color change. This clearly demonstrates that protons are required for the bridge-splitting reaction. A working hypothesis is provided in Scheme 1.

(20) Hubin, T. J.; McCormick, J. M.; Alcock, N. W.; Busch, D. H. *Inorg. Chem.* **2001**, *40*, 435.
(21) (a) Rajendiran, T. M.; Caudle, M. T.; Kirk, M. L.; Setyawati, I.; Kampf, J. W.; Pecoraro, V. L. *J. Biol. Inorg. Chem.* **2003**, *8*, 283. (b) Panja, A.; Shaikh, N.; Gupta, S.; Butcher, R. J.; Banerjee, P. *Eur. J. Inorg. Chem.* **2003**, 1540.
(22) Warzeska, S. T.; Micciche, F.; Mimmi, M. C.; Bouwman, E.; Kooijman, H.; Spek, A. L.; Reedijk, J. *J. Chem. Soc., Dalton Trans.* **2001**, 3507.
(23) Huang, D.; Wang, W.; Zhang, X.; Chen, C.; Chen, F.; Liu, Q.; Liao, D.; Li, L.; Sun, L. *Eur. J. Inorg. Chem.* **2004**, 1454.

Scheme 2

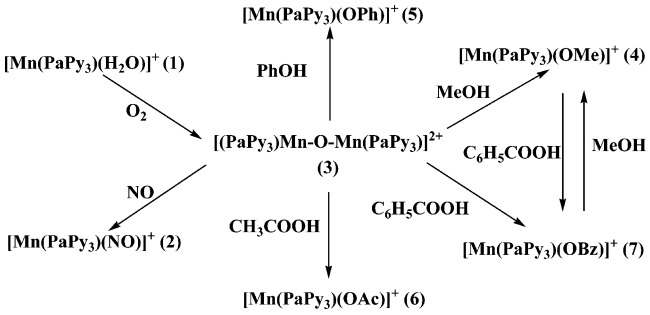

In addition, facile ligand substitution reactions can take place at the labile sixth site in these complexes. For example, simple dissolution of **7** in MeOH results in conversion of **7** into **4**. The reverse reaction takes place when benzoic acid is added to a solution of **4** in MeCN. These reactions are summarized in Scheme 2.

Reductive Nitrosylation. In a previous account, we have reported that the Mn(II) center of **1** with bound carboxamido N readily forms the {Mn−NO}^{6} nitrosyl **2** in the presence of NO.[8] Since passage of NO through a solution of the mononuclear Mn(III) complex [Mn(PaPy$_3$)(MeCN)](ClO$_4$)$_2$ or [Mn(PaPy$_3$)(Cl)](ClO$_4$) did not afford a nitrosyl complex, we suggested that NO only reacts with Mn(II) center in the presence of coordinated carboxamido group(s).[8] Interestingly, in this work, we have discovered that passage of NO through a degassed solution of the (μ-oxo)dimanganese(III) complex **3** in MeCN affords **2** (Scheme 2). It appears that reduction of the Mn(III) centers and concomitant coordination by NO gives rise to the {Mn−NO}^{6} species **2** in such reaction. This reactivity presumably arises from the instability of the single unsupported oxo bridge in **3**. Loss of the bridging oxide from **3** as O atom upon reaction with NO (and formation of NO_2) is the reason for the observed Mn(III) → Mn(II) reduction (eq 1). This mechanism is supported by the fact that when **3** is completely converted into **2** in the presence of NO (as followed by the absorption spectrum of the reaction mixture), one detects 1 equiv of NO_2 in the headspace by GC analysis.

$$[(PaPy_3)Mn{-}O{-}Mn(PaPy_3)]^{2+}\ (\mathbf{3}) \xrightarrow{3NO} 2[Mn(PaPy_3)(NO)]^{+}\ (\mathbf{2}) + NO_2 \quad (1)$$

Another aspect of the reductive nitrosylation reaction must be mentioned here. We have previously shown that NO does not react with the Mn(III) center of either [Mn(PaPy$_3$)(MeCN)](ClO$_4$) or [Mn(PaPy$_3$)(Cl)](ClO$_4$).[8] However, when a strongly basic ligand like (dimethylamino)pyridine (DMAP) or MeO$^-$ is present at the site trans to the coordinated carboxamido nitrogen, NO reacts with such species in MeCN and causes reduction (and binding). In fact, all the mononuclear complexes reported here afford the {Mn−NO}^{6} complex **2** by reductive nitrosylation (eq 2). This reaction provides an additional synthetic route to the photosensitive {Mn−NO}^{6} nitrosyl **2**.

$$\left.\begin{array}{l}[Mn(PaPy_3)(OMe)]^{+}\ (\mathbf{4})\\ [Mn(PaPy_3)(OPh)]^{+}\ (\mathbf{5})\\ [Mn(PaPy_3)(OAc)]^{+}\ (\mathbf{6})\\ [Mn(PaPy_3)(OBz)]^{+}\ (\mathbf{7})\end{array}\right\} \xrightarrow{NO} [Mn(PaPy_3)(NO)]^{+}\ (\mathbf{2}) \quad (2)$$

Metal nitrosyls have been synthesized by reductive nitrosylation in MeOH in the presence of a base (metal:base ratio = 1:1).[24] In the present case, the basic ligands (like OMe and OAc) in **4**−**7** serve as the in-situ base to promote the reductive nitrosylation reaction. The mechanism of this base-initiated reductive nitrosylation has recently been reviewed by Ford and co-workers.[25]

In general, non-porphyrin Mn(III) complexes react with NO to afford EPR-active {Mn−NO}^{5} species. For example, Mn(III) complexes of the type [Mn(Z-SALDPT)(NCS)] (Z-SALDPT = pentadentate Schiff base ligands derived from various salicylaldehydes and triamines) react with NO to yield EPR-active species arising from the transfer of the radical electron from NO to the manganese center.[12] The formation of the non-porphyrin {Mn−NO}^{6} nitrosyl **2** from the various Mn(III) precursors reported here (eqs 1 and 2) is therefore quite unprecedented. In porphyrin chemistry, only a handful of {Mn−NO}^{6} species of the type [(NO)Mn(TPP)(B)] (TPP = tetraphenylporphyrinato ligand, B = piperidine, 4-methylpiperidine, *N*-methylimidazole) has been derived from the Mn(III) starting complex [ClMn(TPP)].[26,27]

In conclusion, [(Mn(PaPy$_3$))$_2$(μ-O)](ClO$_4$)$_2$ (**3**), a dimanganese(III) complex with a single unsupported oxo bridge, has been synthesized and characterized by crystallography. This complex serves as an excellent precursor for mononuclear Mn(III) complexes of the type [Mn(PaPy$_3$)(L)](ClO$_4$), where L is typical anionic O-based ligands such as MeO$^-$ and AcO$^-$. These mononuclear Mn(III) complexes as well as **3** undergo reductive nitrosylation to afford the photosensitive {Mn−NO}^{6} nitrosyl [Mn(PaPy$_3$)NO](ClO$_4$) (**2**).

Acknowledgment. Experimental assistance from Prof. Jeffrey Long and Dr. Hye Jin Choi is gratefully acknowledged. A.A.E.-R. was supported by the NIH ISMD Grant GM58903.

Supporting Information Available: X-ray crystallographic files in CIF format for [(Mn(PaPy$_3$))$_2$(μ-O)](ClO$_4$)$_2$·2.7CH$_2$Cl$_2$·0.5CH$_3$CN (**3**·2.7CH$_2$Cl$_2$·0.5CH$_3$CN), [Mn(PaPy$_3$)(OMe)](ClO$_4$) (**4**), [Mn(PaPy$_3$)(OPh)](ClO$_4$) (**5**), and [Mn(PaPy$_3$)(OBz)](ClO$_4$)·CH$_2$Cl$_2$ (**7**·CH$_2$Cl$_2$). This material is available free of charge via the Internet at http://pubs.acs.org.

IC0503535

(24) Gwost, D.; Caulton, K. G. *Inorg. Chem.* **1973**, *12*, 2095.
(25) Ford, P. C.; Fernandez, B. O.; Lim, M. D. *Chem. Rev.* **2005**, *105*, 2439.
(26) (a) Piciulo, P. L. Rupprecht, G.; Scheidt, W. R. *J. Am. Chem. Soc.* **1974**, *96*, 5293. (b) Piciulo, P. L.; Scheidt, W. R. *Inorg. Nucl. Chem. Lett.* **1975**, *11*, 309.
(27) Zahran, Z. N.; Lee, J.; Alguindigue, S.; Khan, M. A.; Richter-Addo, G. B. *J. Chem. Soc., Dalton Trans.* **2004**, 44.